

Understanding Discrepancies of Wavefunction Theories for Large Molecules

Tobias Schäfer,^{1*} Andreas Irmeler,^{1*} Alejandro Gallo,¹ Andreas Grüneis^{1*}

¹Institute for Theoretical Physics. TU Wien
Wiedner Hauptstraße 8–10/136, Vienna, A-1040, Austria

*Corresponding authors. E-mail: tobias.schaefer@tuwien.ac.at

Quantum mechanical many-electron calculations can predict properties of atoms, molecules and even complex materials. The employed computational methods play a quintessential role in many scientifically and technologically relevant research fields. However, a question of paramount importance is whether approximations aimed at reducing the computational complexity for solving the many-electron Schrödinger equation, are accurate enough. Here, we investigate recently reported discrepancies of noncovalent interaction energies for large molecules predicted by two of the most widely-trusted many-electron theories: diffusion quantum Monte Carlo and coupled-cluster theory. We are able to unequivocally pin down the source of the puzzling discrepancies and present modifications to widely-used coupled-cluster methods needed for more accurate noncovalent interaction energies of large molecules on the hundred-atom scale. This enhances the reliability of predictions from quantum mechanical many-electron theories across a wide range of critical applications, including drug design, catalysis, and the innovation of new functional materials, such as those for renewable energy technologies.

1 Introduction

The prediction of electronic transition energies for a single hydrogen atom in 1926 marks the beginning of an incredible successful era of quantum mechanics (1, 2). Shortly after this breakthrough, Paul Dirac famously noted that the underlying physical laws necessary for much of physics and all of chemistry are now completely known. However, he also pointed out that the exact application of these laws leads to equations that are much too complicated to solve (3). This paradigm of theoretical chemistry and physics is prevalent until today. In particular, the exponential growth of the computational complexity of the many-electron problem with system size still makes an exact solution of the electronic Schrödinger equation for more than a few atoms impossible. As a consequence, a hierarchy of increasingly accurate methods that is capable of producing reference results at the expense of tractable yet high computational cost has emerged. These reference results are pivotal in order to develop, assess, and further improve computationally more efficient but in general less accurate approximations. In this context, a prime example was the numerical prediction of highly accurate ground state energies for the uniform electron gas using diffusion Monte Carlo methods, leveraging the development of approximate exchange-correlation functionals that ultimately led to the breakthrough of density functional theory in computational materials science during the last decades (4–6).

At present, quantum mechanical many-electron calculations of systems containing more than 100 atoms have become possible thanks to methodological developments and considerable growth in computing power. These methodological improvements are often based on taking advantage of the relative short-rangedness of many-electron correlation effects (7–9). In this manner, the scaling of the computational complexity with respect to system size can be lowered. However, recently several works (10–13) showed that there exist alarming discrepancies between predicted interaction energies for large molecules when using two of the most widely-trusted highly accurate many-electron theories: DMC and CCSD(T), which stand for diffusion Monte Carlo and coupled-cluster theory using single, double, and perturbative triple particle-hole excitation operators, respectively. These observations are a source of great concern in the electronic structure theory community because, in the case of noncovalent interactions between molecular complexes, both CCSD(T) and DMC are considered highly reliable benchmark methods (14, 15). Furthermore, the observed discrepancies are large enough to cause qualitative differences in calculated properties of materials, which can have scientific, technological, and even clinical implications. For example, accurate crystal structure predictions are crucial in drug design to differentiate between harmful and effective polymorphs (16–18). Similarly, reliable reference methods are essential for discovering and designing new functional materials for applications such as renewable energy storage and conversion, including catalysis, or

solar cells (19–21). Finally, as machine learning increasingly pervades all areas of computational first-principles physics, the accuracy of these reference methods, which provide the training data, becomes even more critical (22–24).

In the following, we analyze a set of large molecular systems where large discrepancies between approximated versions of DMC and CCSD(T) were observed (10, 11). Importantly, a direct experimental measurement of the computed interaction energies of these systems is complicated and prone to significant uncertainties. Therefore, it is an open challenge to identify the origin of the observed deviations for the employed highly accurate yet approximate theoretical approaches.

2 Results

We present an approach which allows us to unambiguously test if the employed approximations for DMC and CCSD(T) cause the puzzling discrepancies between their predictions. In particular, our methodology exhibits three striking advantages. Firstly, due to its efficient and massive computational parallelization, we omit any local correlation approximation, as was employed for the CCSD(T) calculations in Refs. (11–13). Secondly, we use a plane wave basis set to enable an unbiased assessment of the quality of previously employed tabulated atom-centered basis functions. Thirdly, we are able to study the influence of higher-order contributions to the many-electron perturbation expansion beyond CCSD(T) theory for large molecular complexes.

In order to demonstrate the reliability of our plane wave basis approach, we first investigate the parallel displaced benzene dimer as a benchmark. We find that our approach effectively addresses the challenges of noncovalent interactions between large molecules, combining the compactness and systematic improvability of natural orbitals without near-linear dependencies that plague atom-centered Gaussian basis sets for densely packed structures. As discussed in the supplementary information, our computed CCSD(T) interaction energies for the parallel displaced benzene dimer are in excellent agreement with Gaussian basis set results. Next, we turn to the coronene dimer interaction energy, where significant discrepancies between DMC and CCSD(T) have been observed (10, 11). As shown in Tab. 1, our canonical CCSD(T) estimates for the parallel displaced coronene dimer align closely with domain-based local pair-natural orbital (DLPNO-CCSD(T)) and local natural orbital (LNO-CCSD(T)) results, ruling out basis set incompleteness and local approximation errors as sources of discrepancies with DMC findings. However, it is noteworthy that the CCSD(T) interaction energy contains a large (T) contribution of about -8 kcal/mol, indicating that the correct treatment of triple particle-hole excitation effects for the electronic correlation plays a crucial role.

Table 1: **Interaction energy in kcal/mol of the parallel displaced coronene dimer (C2C2PD) obtained at different levels of theory including MP2, CCSD, CCSD(T), CCSD(cT) and DMC.** The uncertainty of the referenced DMC, LNO and DLPNO results are taken from the corresponding reference. The uncertainty of this work’s results are dominated by the remaining basis set error and the uncertainty of the box size extrapolation.

Theory	Interaction energy	Ref.
MP2	-38.5 ± 0.5	this work
CCSD	-13.4 ± 0.5	this work
CCSD(T)	-21.1 ± 0.5	this work
LNO-CCSD(T)	-20.6 ± 0.6	Ref. (11)
DLPNO-CCSD(T ₀)	-20.9 ± 0.4	Ref. (13)
DMC	-18.1(8)	Ref. (11)
DMC	-17.5(14)	Ref. (10)
CCSD(cT)	-19.3 ± 0.5	this work

2.1 All that glitters is not gold: overcorrelation in CCSD(T)

Having ruled out errors from local approximations and incomplete basis sets for the parallel displaced coronene dimer (C2C2PD), we seek to assess the (T) approximation, which makes a significant contribution to the interaction energy of C2C2PD. In passing we anticipate that the (T) contribution to the interaction energy is also relatively large for all other systems with a significant discrepancy reported in Ref. (11) (see supplementary information).

The (T) approximation was introduced in the seminal work by Raghavachari *et. al.* (25). Since then, it has become one of the most widely-used benchmark methods –sometimes referred to as the ‘gold standard’ of molecular quantum chemistry– for weakly correlated systems. However, we argue that the partly significantly too strong interaction energies in CCSD(T) theory are caused by the employed truncation of the approximation of the triple particle-hole excitation operator. These shortcomings are comparable to the issue of too strong interaction energies from truncated perturbation theories for systems with large polarizabilities, as discussed by Nguyen *et. al.* (26). As can be observed for the coronene dimer in Table 1, second-order Møller-Plesset perturbation theory (MP2)—a truncated perturbation theory—exhibits this overestimation of the interaction energy. In the extreme case of an infinite polarizability, as it occurs in metallic systems, MP2 and CCSD(T) even yield divergent correlation energies in the thermodynamic limit, which is referred to as

infrared catastrophe (27, 28). In contrast, a resummation of certain terms to infinite order can yield interaction energies with an accuracy that is less dependent on the polarizability. Prominent examples for such approaches include the CCSD theory as well as the random-phase approximation. We have recently presented a method, denoted as CCSD(cT), that averts the infrared catastrophe of CCSD(T) by including selected higher-order terms in the triples amplitude approximation without significantly increasing the computational complexity (28).

Understanding the discrepancy

For the present work it is important to note that the main difference between CCSD(cT) and CCSD(T) theory originates from the employed approximation to the triple particle-hole excitation amplitudes. The triple amplitudes of the (cT) approximation are given in diagrammatic and algebraic form by (28)

$$\begin{aligned}
 \text{Diagram 1} &= \text{Diagram 2} + \text{Diagram 3} \\
 t_{ijk}^{abc} &= \langle abc | [\hat{V}, \hat{T}_2] | 0 \rangle + \frac{1}{2i} [[\hat{V}, \hat{T}_2], \hat{T}_2] | 0 \rangle / \Delta_{abc}^{ijk} \quad (1)
 \end{aligned}$$

where \hat{V} and \hat{T}_2 stand for the Coulomb interaction and the double particle-hole excitation operator, respectively. For brevity, the contributions from the single excitation operator are not included and only one additional ‘direct’ diagram is depicted. In here, $\Delta_{abc}^{ijk} = \varepsilon_i + \varepsilon_j + \varepsilon_k - \varepsilon_a - \varepsilon_b - \varepsilon_c$, with ε ’s being one-electron HF energies. The bra- and ket-states correspond to a triple excited and reference state, respectively. The (T) approximation disregards the term $[[\hat{V}, \hat{T}_2], \hat{T}_2]$, which is included in (cT) and also occurs in full CCSDT theory. This term effectively screens the bare Coulomb interaction of the $[\hat{V}, \hat{T}_2]$ term and has an opposite sign, making it crucial for systems with large polarizability. However, for small and weakly polarizable systems the $[[\hat{V}, \hat{T}_2], \hat{T}_2]$ contribution is small, making the (T) and (cT) approximation agree, as it was already shown for a set of small molecules (28).

We now demonstrate that using CCSD(cT) instead of CCSD(T) theory restores excellent agreement for noncovalent interaction energies with DMC findings. First, we consider again the coronene dimer. Table 1 shows that the binding energy for the coronene dimer calculated on the level of CCSD(cT) theory is by almost 2 kcal/mol closer to the DMC estimate compared to CCSD(T) theory, achieving chemical accuracy (1 kcal/mol) in comparison to DMC after subtracting error bars. Next, we investigate the accuracy of CCSD(T) and CCSD(cT) compared to DMC for noncovalent interactions in smaller molecules. To this end, we study a set of dimers containing up to 24 atoms that were also investigated in Ref. (11). This gives us another opportunity to assess the effect of local approximations at the level of CCSD(T) theory. Fig. 1 depicts the deviations of all computed interaction

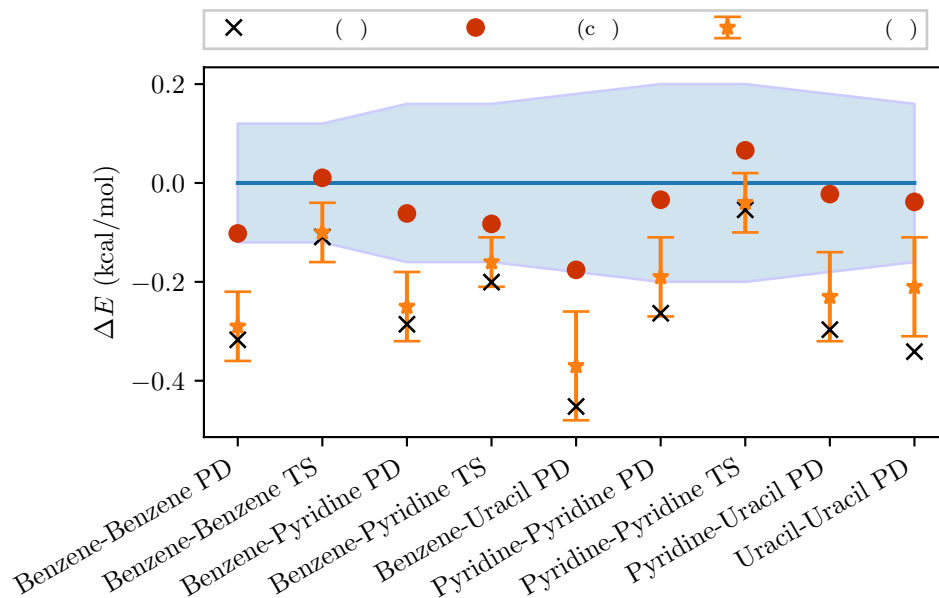


Figure 1: **Deviations of coupled cluster results from DMC results for a set of non-covalently bound dimers with up to 24 atoms.** The CCSD(T) and CCSD(cT) values are CBS estimates obtained from basis set extrapolation using aug-cc-pVTZ and aug-cc-pVQZ basis sets (29, 30) (details in the supplementary information). The LNO-CCSD(T) and DMC data are from Ref. (11). The uncertainty measures are as described in Table 1. The uncertainty of DMC is shown by the blue area.

energies from DMC reference values taken from Ref. (11). It should be noted that DMC references and differences to LNO-CCSD(T) interaction energies are shown with error bars (11). Using our massive computational parallelization approach, we are able to add canonical CCSD(T) interaction energies extrapolated to the CBS limit to the comparison to DMC. For these relatively small molecules, we can employ sufficiently large basis sets, reducing the remaining uncertainty to approximately 0.01 kcal/mol (see supplementary information). Importantly, our canonical CCSD(T) results are in good agreement with LNO-CCSD(T) findings to within its error bars. The only minor exception is observed for the parallel displaced uracil dimer, where canonical CCSD(T) predicts a slightly stronger interaction. A comparison to DMC reveals that CCSD(T) theory predicts on average about 0.3 kcal/mol stronger interaction energies. Based on LNO-CCSD(T) and DMC data alone such a statement cannot be made due to the relatively large and mostly overlapping error bars. However, our well converged canonical CCSD(T) findings allow drawing such conclusions. Only for the T-shaped pyridine and benzene dimers, DMC and CCSD(T) binding energies agree to within the DMC errors. Note that these systems have a smaller (T) contribution to the intereaction energy, compared to the parallel displaced systems. All other systems exhibit small but significant discrepancies between CCSD(T) and DMC results, which is consistent with the even larger discrepancies reported for the larger molecules in Ref. (11). Similar to our findings for the coronene dimer reported in Table 1, Fig. 1 shows that CCSD(cT) interaction energies agree significantly better with DMC values than their CCSD(T) counterparts.

Given the good agreement between DMC and CCSD(cT) for the systems studied above, an important question to ask is if CCSD(cT) is really more accurate than CCSD(T) for noncovalent interaction energies? To answer this question we compare interaction energies of both approaches to higher-level CC methods for complexes from the S22 data set. As can be observed in Fig. 2, we find that while (T) is in good agreement with T for total energies, it overestimates interaction energies. Here T stands for the triples contribution to the correlation energy, $E^T = E^{\text{CCSDT}} - E^{\text{CCSD}}$. (cT) closely matches the T interaction energies, indicating its superior accuracy for weakly bound complexes. This effect is particularly strong for interaction energies with large triples correlation contributions.

2.2 Estimating the overcorrelation of (T) for weak interactions

In summary, we have demonstrated that CCSD(cT) theory achieves excellent agreement for noncovalent interaction energies between molecular complexes compared to DMC and CCSDT theory. However, we stress that the CC series of methods (CCSD, CCSDT and CCSDTQ) is observed to yield monotonic and rapidly converging interaction energies for small and weakly bound complexes (32). Based on this knowledge, we emphasize that

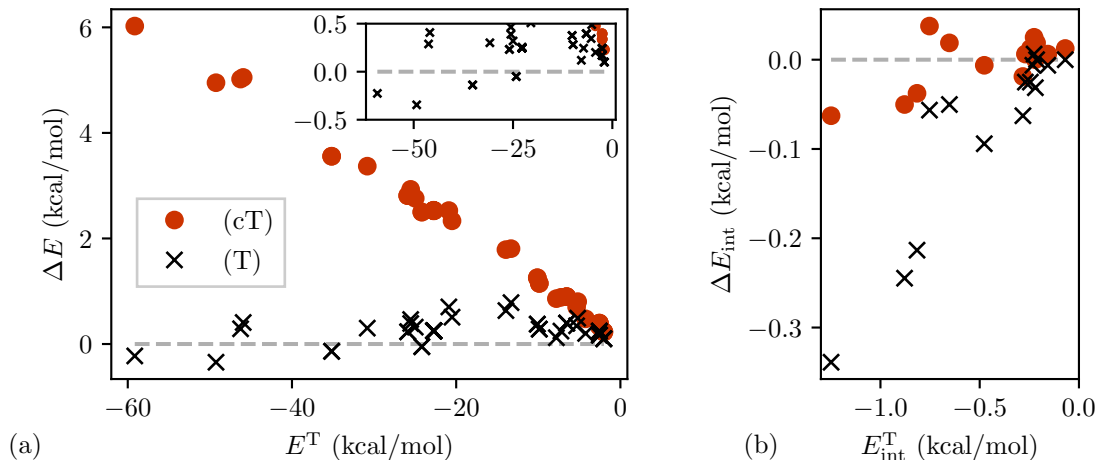


Figure 2: **Comparison between the full triples and the perturbative triples approaches, (cT) and (T) for a set of molecules contained in the S22 data set (31).** The total triples correlation energy contribution E^T on the x-axis is compared to both differences between the (T), (cT) correlation energy contributions and E^T for **a)** total energies and **b)** interaction energies.

the Q contribution to the interaction energies can be expected to be smaller than its T counterpart, but could possibly yield a significant contribution. Indeed, this is part of the reason for the success of the CCSD(T) approximation for very small molecules, where CCSD(T) is often fortuitously closer to CCSDTQ than CCSDT (32). Here, we argue that this error cancellation no longer functions in the case of large molecular complexes involving strongly polarizable systems such as C2C2PD, C3GC and C60@[6]CPPA. A similar problem is known to occur in MP2 theory, where the truncation of the perturbation series also leads to significantly too strong interaction energies for systems with large polarizability, although MP2 yields relatively accurate interaction energies for systems with an intermediate polarizability (26). To quantify and support the statements above, Fig. 3 illustrates that there exists a correlation between the ratio of (T) and (cT) with the ratio of the MP2 and CCSD correlation energy contributions to the interaction energies of all studied molecules in this work with dispersion-dominated interactions. This demonstrates that (T) exhibits a tendency to overestimate the absolute binding energy in a similar manner as MP2 theory for more polarizable systems. Although an overestimation of the (T) binding energy contribution compared to its (cT) counterpart by about 10% might yield a fortuitously better agreement between CCSD(T) and CCSDTQ, we argue that 20–30% overestimation is expected to yield significantly too strong interaction energies. For exam-

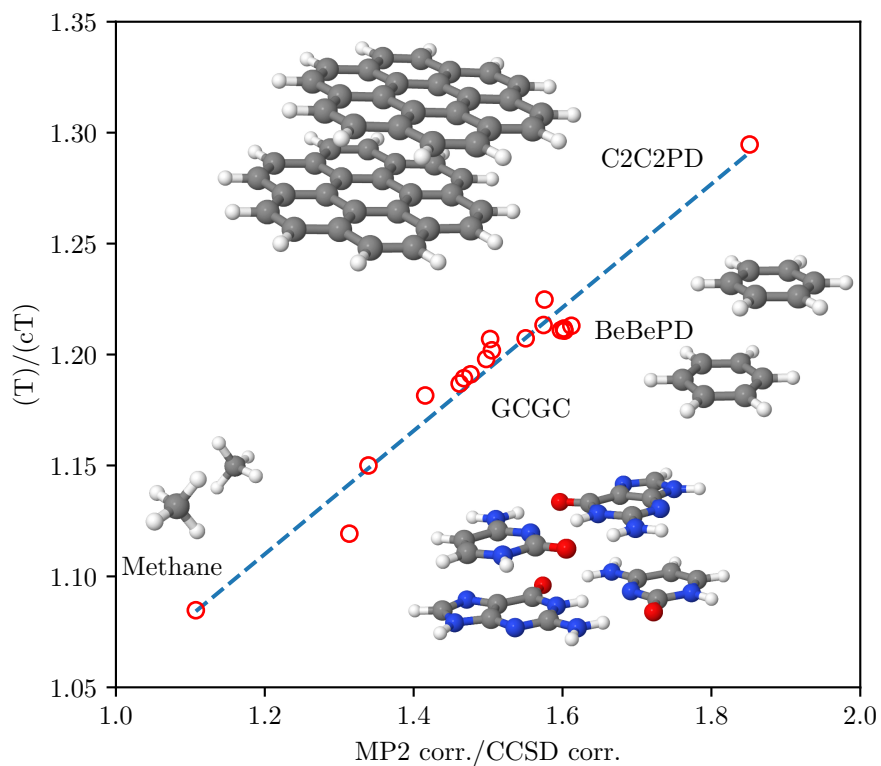


Figure 3: **Correlation between the ratio of (T) and (cT) with the ratio of the MP2 and CCSD correlation energy contributions to interaction energies of a set of dispersion-dominated complexes from the S22, L7 and S66 benchmark datasets (31, 33, 34).** Selected cases are labeled and visualized: Methane dimer, GCGC (guanine-cytosine tetramer), BeBePD (benzene dimer parallel displaced), C2C2PD (coronene dimer parallel displaced). All the data is available in the supplementary information.

Table 2: **Comparison of the interaction energy for large molecular complexes in kcal/mol as calculated by different levels of theory.** Showcasing partially large discrepancies between CCSD(T) and DMC on the one hand, and an excellent agreement between CCSD(cT) and DMC results for complexes up to the 100-atom scale on the other hand. CCSD(T) and CCSD(cT) results are obtained using our plane wave approach. The calculation and the uncertainty of CCSD(cT)-fit is explained in the supplementary information.

System	CCSD(T)	LNO-CCSD(T) (<i>11</i>)	CCSD(cT)	CCSD(cT)-fit	DMC (<i>11</i>)	DMC (<i>10</i>)
GGG	-1.5 ± 0.5	-2.1 ± 0.2	-1.2 ± 0.5	-1.8 ± 0.2	-1.5(6)	-2.0(8)
GCGC	-13.1 ± 0.5	-13.6 ± 0.4	-12.5 ± 0.5	-12.8 ± 0.5	-12.4(8)	-10.6(12)
C2C2PD	-21.1 ± 0.5	-20.6 ± 0.6	-19.3 ± 0.5	-18.9 ± 0.7	-18.1(8)	-17.5(14)
C3A		-16.5 ± 0.8		-15.3 ± 0.9	-15.0(10)	-16.6(18)
PHE		-25.4 ± 0.2		-25.0 ± 0.2	-26.5(13)	-24.9(12)
C3GC		-28.7 ± 1.0		-26.7 ± 1.1	-24.2(13)	-25.1(18)
C ₆₀ @[6]CPPA		-41.7 ± 1.7		-35.6 ± 2.0	-31.1(14)	

ple, the values of (T)/(cT) for the Benzene-Benzene PD and coronene dimer are 1.2 and 1.3, respectively.

Having demonstrated and explained the reasons for the overestimation of absolute interaction energies on the level of CCSD(T) theory for small molecules with up to 24 atoms and the C2C2PD system, we now want to turn to the discussion of the remaining large molecular complexes where significant absolute discrepancies between DMC and CCSD(T) have been observed. These systems include C3GC from the L7 data set and the C60@[6]CPPA buckyball-ring. Here, substantial differences in the binding energies of 2.2 kcal/mol and 7.6 kcal/mol were reported, respectively after subtracting error bars. Although CCSD(cT) calculations for systems of that size are currently not feasible using our approach, we now introduce a simplified model that allows us to estimate the change in interaction energies from CCSD(T) to CCSD(cT) in an approximate manner. Given the linear trend between the different correlation energy contributions to the interaction energy depicted in Fig. 3, it is possible to estimate the (cT) contribution for systems where only MP2, CCSD and (T) are known. These numbers can be calculated using a computationally efficient LNO-CCSD(T) implementation (35). Results computed in this manner are denoted as CCSD(cT)-fit. Details about this procedure and the corresponding error estimates are provided in the supplementary information. Table 2 gives our estimated CCSD(cT) interaction energies in comparison to CCSD(T) and DMC findings for seven large molecular complexes. A comparison between CCSD(cT)-fit and the explicitly calculated CCSD(cT) results for GGG, GCGC and C2C2PD shows that the linear regression model is sufficiently reliable for the systems studied in this work. For comparison Table 2

also summarizes the DMC interaction energies from Refs. (10) and (11), which agree to within at least 1 kcal/mol for GGG, C2C2PD, PHE and C3GC. For the remaining systems the DMC estimates show a larger discrepancy and for C60@[6]CPPA only one DMC estimate is available. Although the DMC binding energies have overlapping error bars, the remaining uncertainties are relatively large, illustrating that obtaining highly accurate interaction energies for these large molecules is also challenging for DMC.

As already discussed in Ref. (11), CCSD(T) interaction energies listed Table 2 exhibit large discrepancies compared to DMC for C2C2PD, C3GC and C60@[6]CPPA. In contrast, CCSD(cT)-fit resolves these discrepancies for all systems on the hundred-atom scale, achieving excellent agreement with DMC estimates of Hamdani *et. al.* (11) to within chemical accuracy (1 kcal/mol) after subtracting the error bars. Even for C60@[6]CPPA, which contains 132 atoms, a discrepancy of only 1.1 kcal/mol remains, although the error bar of CCSD(cT)-fit is relatively large in this case. We argue that the remaining discrepancies are potentially caused by uncertainties in DMC, CCSD(cT)-fit and the underlying LNO-CCSD(T) calculations. It should be noted that the error bars of LNO-CCSD(T) interaction energies are in some cases underestimated, as exemplified for the Uracil-Uracil PD dimer by the comparison between canonical CCSD(T) and LNO-CCSD(T) interaction energies shown in Fig. 1. Furthermore, the DMC interaction energy of C60@[6]CPPA has not yet been verified independently using a different DMC implementation as it was done for all other systems listed in Table 2. We also stress that in some cases the differences between the DMC estimates are larger than their respective error bars.

3 Conclusion

Our work unequivocally demonstrates that, due to the employed truncation of the many-body perturbation series expansion, one of the most widely-used and accurate quantum chemistry approaches – CCSD(T) theory – in certain cases binds noncovalently interacting large molecular complexes too strongly. Our findings show that a simple yet efficient modification denoted as CCSD(cT) remedies these shortcomings. This paves the way for highly reliable benchmark calculations of large molecular complexes on the hundred-atom scale that play a crucial role in scientific and technological problems, for example, drug design and surface science. We stress that the more accurate CCSD(cT) approximation can directly be transferred to computationally efficient low-scaling and local correlation approaches, which will substantially advance the applications of theoretical chemistry as well as physics in all areas of computational materials science where highly accurate benchmark results are urgently needed. We are witnessing an unremitting expansion of the frontiers of accurate electronic structure theories to ever larger systems which when

combined with machine-learning techniques, has the potential to transform the paradigm of modern computational materials science.

References

1. E. Schrödinger, *Annalen der Physik* **384**, 361 (1926).
2. W. Pauli, *Zeitschrift für Physik* **36**, 336 (1926).
3. P. A. M. Dirac, *Proceedings of the Royal Society of London Series A* **123**, 714 (1929).
4. W. Kohn, L. J. Sham, *Phys. Rev.* **140**, A1133 (1965).
5. D. M. Ceperley, B. J. Alder, *Phys. Rev. Lett.* **45**, 566 (1980).
6. R. O. Jones, *Rev. Mod. Phys.* **87**, 897 (2015).
7. C. Riplinger, B. Sandhoefer, A. Hansen, F. Neese, *The Journal of chemical physics* **139** (2013).
8. Q. Ma, H.-J. Werner, *Journal of Chemical Theory and Computation* **15**, 1044 (2019).
9. P. B. Szabó, J. Csóka, M. Kállay, P. R. Nagy, *Journal of Chemical Theory and Computation* **19**, 8166 (2023).
10. A. Benali, H. Shin, O. Heinonen, *The Journal of Chemical Physics* **153**, 194113 (2020).
11. Y. S. Al-Hamdani, *et al.*, *Nature Communications* **12**, 3927 (2021).
12. F. Ballesteros, S. Dunivan, K. U. Lao, *The Journal of Chemical Physics* **154**, 154104 (2021).
13. C. Villot, F. Ballesteros, D. Wang, K. U. Lao, *The Journal of Physical Chemistry A* **126**, 4326 (2022).
14. J. Řezáč, P. Hobza, *Chemical Reviews* **116**, 5038 (2016).
15. M. Dubecký, L. Mitas, P. Jurečka, *Chemical Reviews* **116**, 5188 (2016).
16. D. Firaha, *et al.*, *Nature* **623**, 324 (2023).
17. J. Hoja, *et al.*, *Science Advances* **5**, eaau3338 (2019).

18. A. M. Reilly, *et al.*, *Acta Crystallographica Section B: Structural Science, Crystal Engineering and Materials* **72**, 439 (2016).
19. L. Chanussot, *et al.*, *ACS Catalysis* **11**, 6059 (2021).
20. J. Sauer, *Journal of Catalysis* **433**, 115482 (2024).
21. M. Bokdam, J. Lahnsteiner, B. Ramberger, T. Schäfer, G. Kresse, *Physical Review Letters* **119**, 145501 (2017).
22. A. G. Donchev, *et al.*, *Scientific Data 2021 8:1* **8**, 1 (2021).
23. P. Eastman, *et al.*, *Scientific Data 2022 10:1* **10**, 1 (2023).
24. P. Liu, *et al.*, *Physical Review Letters* **130**, 078001 (2023).
25. K. Raghavachari, G. W. Trucks, J. A. Pople, M. Head-Gordon, *Chemical Physics Letters* **157**, 479 (1989).
26. B. D. Nguyen, *et al.*, *Journal of Chemical Theory and Computation* **16**, 2258 (2020).
27. J. J. Shepherd, A. Grüneis, *Phys. Rev. Lett.* **110**, 226401 (2013).
28. N. Masios, A. Irmeler, T. Schäfer, A. Grüneis, *Phys. Rev. Lett.* **131**, 186401 (2023).
29. J. Dunning, Thom H., *The Journal of Chemical Physics* **90**, 1007 (1989).
30. R. A. Kendall, T. H. Dunning, R. J. Harrison, *J. Chem. Phys.* **96**, 6796 (1992).
31. P. Jurečka, J. Šponer, J. Černý, P. Hobza, *Phys. Chem. Chem. Phys.* **8**, 1985 (2006).
32. D. G. A. Smith, P. Jankowski, M. Slawik, H. A. Witek, K. Patkowski, *Journal of Chemical Theory and Computation* **10**, 3140 (2014).
33. R. Sedlak, *et al.*, *Journal of Chemical Theory and Computation* **9**, 3364 (2013).
34. J. Řezáč, K. E. Riley, P. Hobza, *Journal of Chemical Theory and Computation* **7**, 2427 (2011).
35. M. Kállay, *et al.*, *The Journal of Chemical Physics* **152**, 074107 (2020).

Acknowledgments

Tobias Schäfer acknowledges support from the Austrian Science Fund (FWF) [DOI: 10.55776/ESP335]. The computational results presented have been largely achieved using the Vienna Scientific Cluster (VSC). Andreas Irmeler and Alejandro Gallo acknowledge support from the European Union's Horizon 2020 research and innovation program under Grant Agreement No. 951786 (The NOMAD CoE). Support and funding from the European Research Council (ERC) (Grant Agreement No. 101087184) is gratefully acknowledged. We gratefully acknowledge discussions with Adrian Daniel Boese.

Supplementary materials

Materials and Methods

Supplementary Text

Figs. S1 to S2

Tables S1 to S5

Supplementary information for: Understanding Discrepancies of Wavefunction Theories for Large Molecules

Tobias Schäfer,* Andreas Irmeler, Alejandro Gallo, and Andreas Grüneis
*Institute for Theoretical Physics, TU Wien,
Wiedner Hauptstraße 8-10/136, 1040 Vienna, Austria*

CONTENTS

S1. Supplementary information notes	1
S2. Selected S66 systems - canonical CBS estimates	1
S3. Selected S22 systems - CCSDT using cc-pVDZ basis sets	3
S4. The plane wave based workflow	4
Benzene dimer (parallel displaced)	4
Coronene dimer (parallel displaced)	4
S5. Estimating CCSD(cT)-fit and its uncertainty	6
Supplementary References	7

S1. SUPPLEMENTARY INFORMATION NOTES

- The CBS estimates for benzene-benzene PD (used in Fig. 1) and the Gaussian basis CCSD(T) estimate of -2.70 kcal/mol are presented in section S2. Furthermore, the CBS estimates for CCSD(T) and CCSD(cT) shown in Fig. 2 can be found in section S2. These numbers are from counterpoise corrected calculations from AVQZ Hartree-Fock calculations together with correlation calculations using a [34] extrapolation. All values are provided in Table S I
- Results depicted in Fig. 3 for molecules contained in the S22 data set on the level of T, (T) and (cT) theory are summarized in S3
- The plane wave approach used for the results in Fig. 1, Table 1, Fig. 4, and Table 2 is explained section S4
- Results for (T) energy contributions of the large molecular systems mentioned in Section 2.2 can be found in Table S V
- The fitting procedure in Section 2.3 is explained in section S5
- Data used in Fig. 4 is summarized in Table S IV

S2. SELECTED S66 SYSTEMS - CANONICAL CBS ESTIMATES

Here we provide highly accurate CBS estimates using Gaussian type orbitals for 9 molecules from the S66 test set. For Gaussian type orbitals there exists a well established strategy to reach the complete basis set limit (CBS). We use Dunning's correlation consistent basis sets of type aug-cc-pVXZ (AVXZ), where X refers to the cardinal number of the basis set. In this work, we employ X = T, Q, and 5. CBS estimates in post-Hartree-Fock methods are obtained by a two point extrapolation assuming a X^{-3} convergence. The extrapolation using AVTZ and AVQZ is denoted as [34], whereas [45] employs the basis sets AVQZ and AV5Z.

Table S I shows the convergence of the interaction energies of the studied molecules with respect to the employed basis set. Results are given for Hartree-Fock, as well as for MP2, CCSD, (T) and the (cT) contribution. Correlation energies were obtained using the MRCC [1] interfaced to our Cc4s code [2].

For these systems, we are able to calculate canonical MP2 results with the AVTZ, AVQZ, and AV5Z basis. One can see that the counterpoise corrected (CP) and the uncorrected (NC) results agree well when the largest available basis set is used. For HF the CP and NC with the AV5Z deviate only by 0.009 kcal/mol or 0.014 kcal/mol for root mean square deviation (rms) and maximal deviation (max), respectively. For MP2 the best available estimate for the complete basis set would be the [45] extrapolation. Here CP and NC deviate by 0.076 and 0.117 kcal/mol rms and max, respectively. It can be seen that results from

* tobias.schaefer@tuwien.ac.at

smaller basis sets are significantly better for CP than for the uncorrected case. For HF the CP corrected results using AVQZ and AV5Z are for all intents and purposes identical, with a maximum deviation of 0.002 kcal/mol. In the NC case AVQZ and AV5Z differ by 0.064 and 0.109 kcal/mol for rms and max, respectively. The same can be observed for MP2, here for the CP results the [34] result is already very close to the [45] value, namely 0.007 and 0.017 kcal/mol for rms and max, respectively. NC results show a larger deviation of 0.112 and 0.250 kcal/mol for rms and max, respectively.

These results allow to conclude that both, AVQZ for HF and [34] extrapolation for MP2, are sufficiently accurate for the given set of systems.

Now we can turn to the CCSD(T) correlation energies. As the BSIE of CCSD(T) is known to be equal and mostly even smaller than in MP2, the provided results obtained from [34] extrapolation are expected to be very close to the CBS. Consequently, the expected deviations from the CBS limit are in the order of 0.01 kcal/mol or lower. These findings are in accordance with CBS estimates from Nagy et al. [3] for the same system using slightly smaller basis sets.

Table S I: Interaction energies in kcal/mol of the studied molecular systems with different Gaussian basis sets. Shown is the Hartree–Fock energy contribution as well as the canonical correlation energies for MP2, CCSD, (T), and (cT). Both counterpoise (CP) corrected results as well as results without CP are presented.

	Method	CP corrected					CP uncorrected				
		AVTZ	AVQZ	AV5Z	[34]	[45]	AVTZ	AVQZ	AV5Z	[34]	[45]
Pyridine-pyridine PD	HF	3.336	3.332	3.331	-	-	3.112	3.273	3.324	-	-
	MP2 corr.	-9.100	-9.238	-9.287	-9.339	-9.339	-10.203	-9.717	-9.503	-9.362	-9.279
	CCSD corr.	-5.673	-5.743	-	-5.794	-	-6.597	-6.061	-	-5.670	-
	(T)	-1.254	-1.286	-	-1.310	-	-1.341	-1.321	-	-1.307	-
	(cT)	-1.029	-1.059	-	-1.080	-	-1.114	-1.093	-	-1.078	-
Pyridine-pyridine TS	HF	0.869	0.867	0.867	-	-	0.703	0.822	0.861	-	-
	MP2 corr.	-5.054	-5.172	-5.213	-5.258	-5.255	-6.016	-5.581	-5.400	-5.263	-5.211
	CCSD corr.	-3.457	-3.538	-	-3.597	-	-4.267	-4.267	-	-3.479	-
	(T)	-0.727	-0.747	-	-0.762	-	-0.801	-0.776	-	-0.758	-
	(cT)	-0.609	-0.628	-	-0.642	-	-0.682	-0.657	-	-0.639	-
Benzene-pyridine PD	HF	3.621	3.619	3.618	-	-	3.395	3.559	3.610	-	-
	MP2 corr.	-8.838	-8.962	-9.006	-9.052	-9.053	-9.991	-9.439	-9.223	-9.036	-8.996
	CCSD corr.	-5.552	-5.609	-	-5.651	-	-6.523	-5.925	-	-5.488	-
	(T)	-1.229	-1.260	-	-1.282	-	-1.320	-1.295	-	-1.277	-
	(cT)	-1.009	-1.038	-	-1.058	-	-1.098	-1.072	-	-1.054	-
Benzene-pyridine TS	HF	0.943	0.943	0.943	-	-	0.745	0.896	0.936	-	-
	MP2 corr.	-4.936	-5.042	-5.079	-5.119	-5.119	-6.016	-5.473	-5.273	-5.077	-5.063
	CCSD corr.	-3.369	-3.438	-	-3.488	-	-4.288	-3.725	-	-3.315	-
	(T)	-0.702	-0.721	-	-0.735	-	-0.786	-0.752	-	-0.728	-
	(cT)	-0.587	-0.605	-	-0.618	-	-0.668	-0.635	-	-0.611	-
Pyridine-uracil PD	HF	2.074	2.072	2.071	-	-	1.730	1.984	2.060	-	-
	MP2 corr.	-10.358	-10.556	-10.631	-10.701	-10.710	-11.935	-11.262	-10.945	-10.770	-10.613
	CCSD corr.	-6.097	-7.024	-	-7.110	-	-8.266	-7.516	-	-6.969	-
	(T)	-1.567	-1.607	-	-1.637	-	-1.692	-1.658	-	-1.634	-
	(cT)	-1.298	-1.335	-	-1.362	-	-1.421	-1.386	-	-1.360	-
Benzene-benzene PD	HF	3.964	3.961	3.960	-	-	3.739	3.901	3.952	-	-
	MP2 corr.	-8.479	-8.587	-8.625	-8.665	-8.666	-9.654	-9.052	-8.837	-8.613	-8.610
	CCSD corr.	-5.350	-5.392	-	-5.423	-	-6.345	-5.699	-	-5.227	-
	(T)	-1.183	-1.212	-	-1.234	-	-1.276	-1.247	-	-1.226	-
	(cT)	-0.973	-0.999	-	-1.019	-	-1.063	-1.033	-	-1.012	-
Benzene-benzene TS	HF	1.448	1.447	1.448	-	-	1.251	1.400	1.440	-	-
	MP2 corr.	-5.030	-5.125	-5.158	-5.194	-5.193	-6.158	-5.554	-5.352	-5.114	-5.141
	CCSD corr.	-3.419	-3.476	-	-3.518	-	-4.385	-3.762	-	-3.308	-
	(T)	-0.715	-0.734	-	-0.748	-	-0.802	-0.765	-	-0.738	-
	(cT)	-0.598	-0.616	-	-0.628	-	-0.682	-0.646	-	-0.620	-
Uracil-uracil PD	HF	0.388	0.379	0.377	-	-	-0.091	0.254	0.363	-	-
	MP2 corr.	-11.047	-11.323	-11.430	-11.525	-11.542	-13.152	-12.298	-11.872	-11.675	-11.425
	CCSD corr.	-7.802	-7.998	-	-8.142	-	-9.660	-8.700	-	-8.000	-
	(T)	-1.887	-1.936	-	-1.972	-	-2.052	-2.006	-	-1.972	-
	(cT)	-1.590	-1.636	-	-1.669	-	-1.751	-1.704	-	-1.670	-
Benzene-uracil PD	HF	3.444	3.443	3.442	-	-	3.070	3.352	3.431	-	-
	MP2 corr.	-10.658	-10.845	-10.914	-10.982	-10.987	-12.348	-11.566	-11.232	-10.996	-10.882
	CCSD corr.	-7.158	-7.260	-	-7.334	-	-8.620	-7.759	-	-7.131	-
	(T)	-1.598	-1.640	-	-1.670	-	-1.732	-1.692	-	-1.664	-
	(cT)	-1.327	-1.366	-	-1.394	-	-1.457	-1.417	-	-1.389	-

S3. SELECTED S22 SYSTEMS - CCSDT USING CC-PVDZ BASIS SETS

Here we provide the numerical data for 15 out of 22 molecular systems from the S22 benchmark set. Results are shown for canonical calculations using the cc-pVDZ basis set. The HF calculations were performed using NWChem [4] and for the post-HF methods we employed an interface to our Cc4s code [5]. Interaction energies shown in the manuscript are evaluated from data summarized in Table II and are not counterpoise corrected.

Table S II: Results for molecular systems of the S22 dataset using the cc-pVDZ basis set in Hartree units. T correlation energy contribution is evaluated via CCSDT-CCSD. The *index* column denotes the identifier of the molecule in the S22 dataset. The *Type* column describes the type of system that has been computed, F1, F2 being the separate fragments, whereas Full denotes the whole system.

Index	System	Type	HF	MP2 corr.	CCSD corr.	(T)	(cT)	T
1	Ammonia dimer	F1	-56.195616	-0.186397	-0.202634	-0.003802	-0.003531	-0.004072
		F2	-56.195616	-0.186397	-0.202634	-0.003802	-0.003531	-0.004072
		Full	-112.396243	-0.375576	-0.407333	-0.007953	-0.007378	-0.008498
2	Water dimer	F1	-76.026603	-0.201874	-0.211441	-0.003051	-0.002844	-0.003214
		F2	-76.026710	-0.201741	-0.211310	-0.003041	-0.002835	-0.003203
		Full	-152.062536	-0.406176	-0.424477	-0.006434	-0.005987	-0.006755
3	Formicacid dimer	F1	-188.778390	-0.500591	-0.512818	-0.015288	-0.013906	-0.015736
		F2	-188.778390	-0.500591	-0.512818	-0.015288	-0.013906	-0.015736
		Full	-377.586256	-1.005708	-1.028426	-0.031867	-0.028964	-0.032677
4	Formamide dimer	F1	-168.945898	-0.483914	-0.502205	-0.015525	-0.014134	-0.016126
		F2	-168.945898	-0.483914	-0.502205	-0.015525	-0.014134	-0.016126
		Full	-337.916259	-0.972313	-1.007590	-0.032177	-0.029269	-0.033301
8	Methane dimer	F1	-40.198702	-0.161179	-0.184661	-0.003702	-0.003457	-0.004092
		F2	-40.198702	-0.161179	-0.184661	-0.003702	-0.003457	-0.004092
		Full	-80.396906	-0.323344	-0.370213	-0.007506	-0.007007	-0.008291
9	Ethene dimer	F1	-78.039915	-0.274850	-0.305009	-0.009796	-0.008999	-0.010426
		F2	-78.039915	-0.274850	-0.305009	-0.009796	-0.008999	-0.010426
		Full	-156.079311	-0.552564	-0.612197	-0.019981	-0.018347	-0.021231
10	Benzene-Methane complex	F1	-230.722189	-0.782664	-0.822131	-0.035812	-0.032184	-0.036209
		F2	-40.198646	-0.161040	-0.184473	-0.003686	-0.003442	-0.004074
		Full	-270.919640	-0.947566	-1.009489	-0.039973	-0.036041	-0.040713
11	Benzene dimer PD	F1	-230.722178	-0.782673	-0.822141	-0.035811	-0.032184	-0.036209
		F2	-230.722178	-0.782673	-0.822141	-0.035811	-0.032184	-0.036209
		Full	-461.437753	-1.578592	-1.652826	-0.073256	-0.065721	-0.073716
12	Pyrazine dimer	F1	-262.702440	-0.835880	-0.862195	-0.038626	-0.034562	-0.038549
		F2	-262.702461	-0.835842	-0.862162	-0.038618	-0.034555	-0.038541
		Full	-525.400639	-1.686240	-1.733417	-0.079039	-0.070599	-0.078493
14	Indolebenzene complex stack	F1	-361.497850	-1.205004	-1.245524	-0.056259	-0.050375	-0.056045
		F2	-230.722148	-0.782743	-0.822212	-0.035828	-0.032199	-0.036226
		Full	-592.211534	-2.007890	-2.080529	-0.094617	-0.084658	-0.094258
16	Etheneethyne complex	F1	-78.039902	-0.274863	-0.305019	-0.009799	-0.009002	-0.010430
		F2	-76.825504	-0.256064	-0.273040	-0.011148	-0.010133	-0.011540
		Full	-154.866735	-0.532540	-0.579048	-0.021214	-0.019372	-0.022218
17	Benzenewater complex	F1	-230.722144	-0.782775	-0.822245	-0.035841	-0.032210	-0.036238
		F2	-76.026578	-0.202033	-0.211581	-0.003066	-0.002859	-0.003230
		Full	-306.751679	-0.987721	-1.035750	-0.039306	-0.035417	-0.039820
18	Benzeneammonia complex	F1	-230.722166	-0.782716	-0.822185	-0.035825	-0.032196	-0.036222
		F2	-56.195676	-0.186468	-0.202699	-0.003821	-0.003548	-0.004091
		Full	-286.918481	-0.972582	-1.027292	-0.040078	-0.036121	-0.040699
19	BenzeneHCN complex	F1	-230.722122	-0.782834	-0.822305	-0.035856	-0.032224	-0.036253
		F2	-92.881359	-0.287354	-0.295666	-0.012245	-0.011064	-0.012427
		Full	-323.607430	-1.074022	-1.120179	-0.048653	-0.043758	-0.049131
20	Benzene dimer TS	F1	-230.722171	-0.782715	-0.822184	-0.035823	-0.032194	-0.036221
		F2	-230.722165	-0.782736	-0.822205	-0.035829	-0.032200	-0.036227
		Full	-461.443197	-1.572462	-1.649192	-0.072557	-0.065161	-0.073207

S4. THE PLANE WAVE BASED WORKFLOW

In this section, the workflow to calculate interaction energies of large molecules in a plane wave basis under periodic boundary conditions is described. All calculations are performed with the Vienna Ab-Initio Simulation Package (VASP) [6] and the Cc4s [7] code.

1. A fixed box size and a plane-wave basis set size are chosen. The scheme is repeated for increasing box sizes to reach the infinite box size limit corresponding to the isolated molecule in the gas phase. The plane-wave basis set size was set via an energy cutoff of 700 eV (ENCUT flag in VASP). This choice resulted from a careful convergence test of the direct-MP2 correlation energy of the coronene dimer, achieving an accuracy well below 0.1 kcal/mol for a fixed box size.
2. The Hartree-Fock ground state is calculated using the given setting. Both the occupied as well as all unoccupied orbitals and orbital energies are stored.
3. Approximate natural orbitals at the MP2 level are calculated, as outlined in Ref. [8]. Natural orbitals are the eigenvectors of the one-electron reduced density matrix. The corresponding eigenvalues are called occupation numbers. Ordered by their occupation number, we truncated and recanonicalized the natural orbital basis by choosing a ratio N_v/N_o , where N_o is the number of occupied orbitals in the system and N_v is the number of chosen natural orbitals. The natural orbitals provide a basis which allows for a much more rapid convergence of the correlation energy with respect to N_v .
4. The MP2 energy is calculated in the CBS limit using the natural orbitals with $N_v/N_o = 200$. This is necessary for basis set correction schemes to estimate the CBS limit of the CCSD and (T) energies. The basis set correction scheme, called focal point correction, is described in Ref. [5].
5. To prepare the coupled cluster calculations a basis of $N_v/N_o = 15$ is chosen. All Coulomb integrals, V_{sr}^{pq} , needed by coupled cluster theory are computed using the expression

$$V_{sr}^{pq} = \sum_{F=1}^{N_F} \Gamma_s^{*pF} \Gamma_{rF}^q, \quad (1)$$

where p, q, r, s refer to occupied or virtual orbital indices. F denotes an auxiliary basis functions, obtained by a singular value decomposition outlined in Ref. [9]. Due to the large vacuum in the simulation cells, significant reductions of the auxiliary basis set size are possible without compromising the precision of computed correlation energies. The correlation energies are converged to within meV with respect to the size of the optimized auxiliary basis set.

6. The final coupled cluster calculations at the level of CCSD, CCSD(T), and CCSD(cT) are performed with our high-performance code called Cc4s. We employed up to 50 compute nodes with 128 cores each to run our massive computational parallelization approach.

Benzene dimer (parallel displaced)

We demonstrate that our plane wave basis approach works reliable for the study of noncovalent interactions between molecules and combines the best of two worlds: compactness and systematic improvability without linear dependencies. To this end we discuss the computed interaction energy of the parallel displaced benzene dimer on the level of CCSD(T) theory and compare to results from basis set converged Gaussian calculations. The total CCSD(T) energy is composed of three terms, the HF total energy, the CCSD correlation energy and the perturbative triples contribution which we denote as (T). Fig. S1(a) depicts the convergence of the CCSD and (T) correlation energy contributions to the computed CCSD(T) interaction energy for a fixed box size with respect to the number of basis functions (natural orbitals) per occupied state (N_v/N_o). We include a recently introduced correction to accelerate the convergence of correlation energies to the complete basis set limit (CBS) [5]. Our findings show that a basis set size of $N_v/N_o = 15$ suffices to achieve convergence to within a fraction of 0.1 kcal/mol. We employ this basis set to compute the CCSD(T) interaction energies and its Hartree-Fock (HF), CCSD and (T) correlation energy contributions for different simulation cell sizes. Fig. S1(b) shows that these contributions converge rapidly. Our fully converged estimate of the CCSD(T) interaction energy for the parallel displaced benzene dimer is -2.62 kcal/mol, which is in excellent agreement with results obtained using Gaussian basis sets of -2.70 kcal/mol.

Coronene dimer (parallel displaced)

Using the example of the coronene dimer (C2C2PD), Fig. S2 shows the dependence of the interaction energy on the box size. The interaction energy exhibits an exponential convergence of the form $a + b \cdot e^{-cV^{1/3}}$, where V is the volume of the box. This behavior holds for both the HF and correlation contributions. The reliability of this extrapolation law is supported by RPA (random phase approximation) calculations of the correlation energy for volumes up to $\sim 5000\text{\AA}^3$. This allows us to converge the interaction energy with a remaining uncertainty of less than 0.5 kcal/mol.

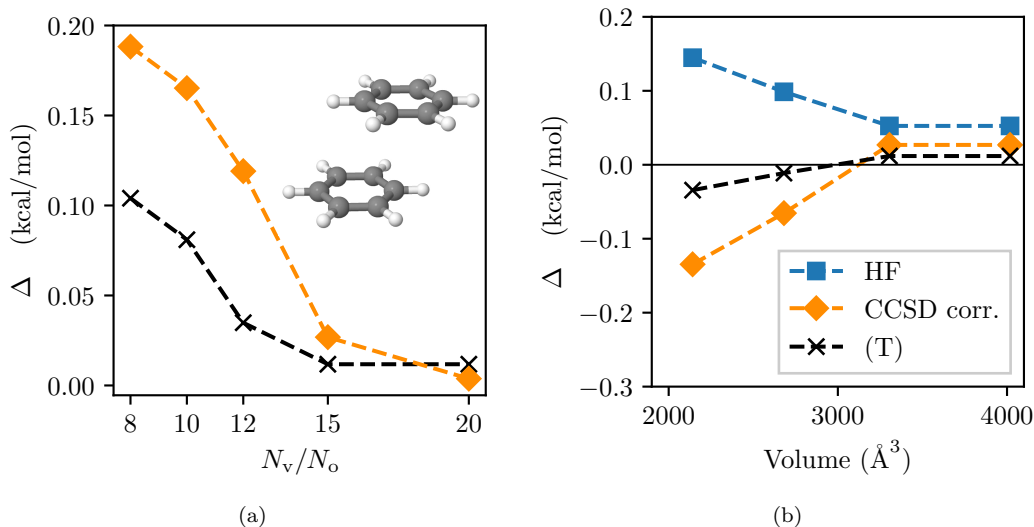


Fig. S 1. **Convergence behavior of the interaction energy for the benzene parallel displaced dimer system.** ΔE is the difference between our plane wave based approach and the reference results from Gaussian basis calculations extrapolated to the CBS limit. **a**, shows the convergence with respect to the number of natural orbitals for a fixed volume of about 4018\AA^3 . **b**, displays the convergence with respect to the volume of the simulation cell with a fixed number of natural orbitals of $N_v/N_o = 15$.

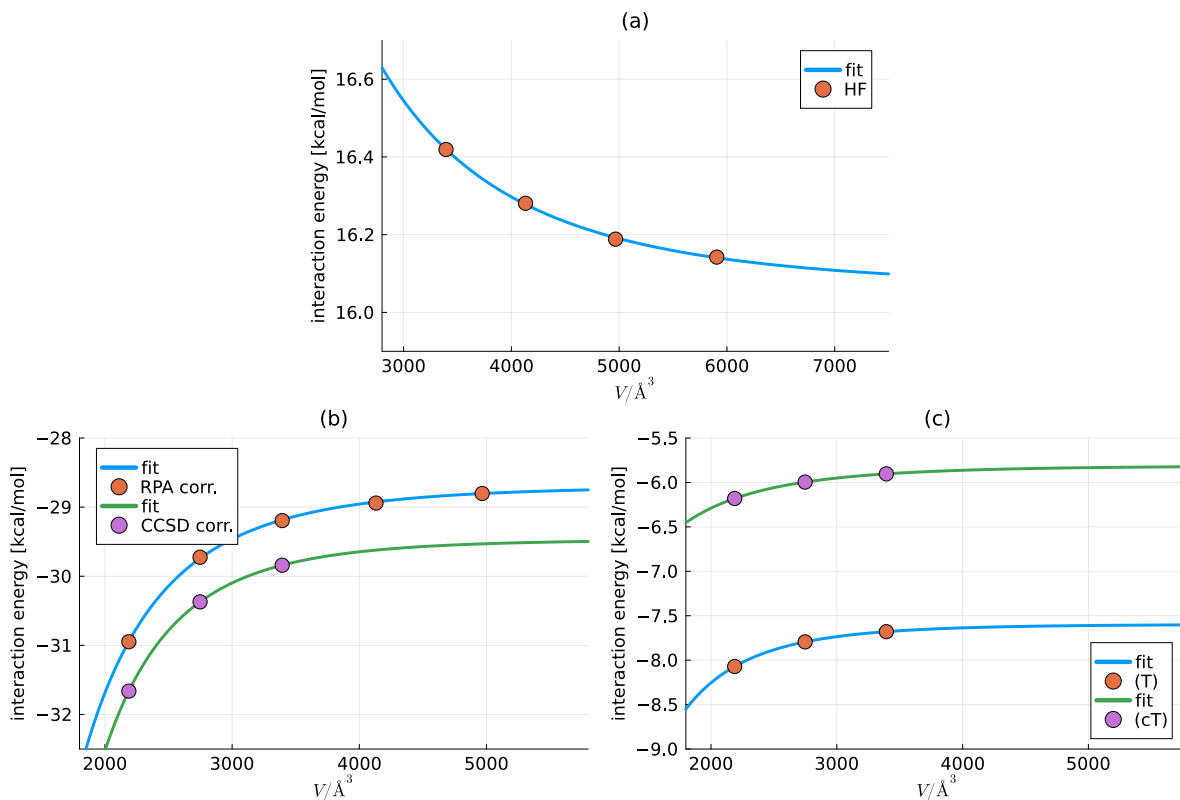


Fig. S 2. Box size dependence of the interaction energy of the coronene dimer for (a) HF, (b) CCSD, and the (c) triples. The CCSD and triples contribution was calculated with a basis set of $N_v/N_o = 15$ and $N_v/N_o = 12$, respectively.

The basis set dependence of the interaction energy is shown in Fig. S2. The additional focal point correction [5] dramatically reduces the basis set error of the CCSD energy and allows us to consider $N_v/N_o = 15$ as a very good approximation to the complete basis set limit. The triples contributions (T) and (cT) are corrected by rescaling the finite basis set result with a factor estimated on the level of MP2 theory as outlined in Ref [10]. Final CBS estimates of interaction energies for three systems in the L7 test set are provided in Table S III.

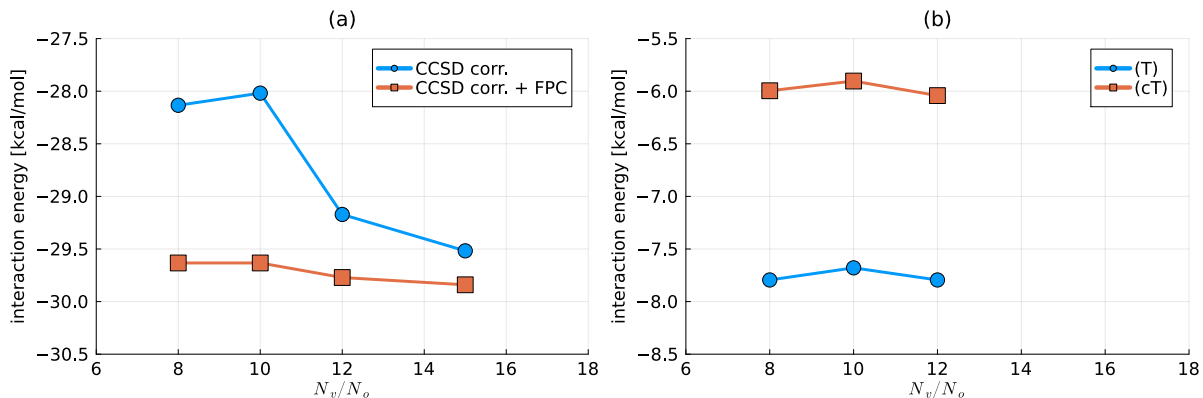


Fig. S 3. Basis set convergence of the correlation contribution of the interaction energy of the coronene dimer at the level of (a) CCSD and the (b) triples. A box size of 3375 \AA^3 was considered. FPC denotes a basis set correction scheme cited in the text.

Table S III. Results of interaction energies in kcal/mol for three molecules from the L7 test set. CBS estimates obtained using the plane wave workflow as described in the text. LNO-CCSD(T) from GTO from literature are provided for comparison.

System	HF	MP2 corr.	CCSD corr.	(T)	(cT)	CCSD(T)	LNO-CCSD(T) [11]
GGG	7.725	-12.245	-7.771	-1.384	-1.130	-1.430	-2.1 ± 0.2
GCGC	12.407	-31.847	-21.193	-4.035	-3.343	-12.821	-13.6 ± 0.4
C2C2PD	16.096	-54.561	-29.471	-7.702	-5.949	-21.077	-20.6 ± 0.6

S5. ESTIMATING CCSD(cT)-FIT AND ITS UNCERTAINTY

As presented in Fig. 4 in the article, a linear trend can be observed, when plotting the ratio of (T) and (cT) against the ratio of the MP2 and CCSD correlation contribution of the interaction energies. The corresponding (T), (cT), MP2 as well as CCSD correlation energy contributions can be found in Table S IV.

A linear fit

$$\frac{(T)}{(cT)} = a + b \cdot \frac{\text{MP2 corr.}}{\text{CCSD corr.}}, \quad (2)$$

gives $a = 0.7764$ and $b = 0.2780$ with a standard deviation of the residuals of $\sigma = 0.0097$. Using this linear relationship, we derive the estimate CCSD(cT)-fit for the interaction energy of large molecules via

$$\text{CCSD}(cT)\text{-fit} = \text{LNO-CCSD} + \frac{1}{X} \cdot \text{LNO-(T)}, \quad (3)$$

where $X = a + b \cdot Y$ and Y is the ratio of the MP2 and CCSD correlation contribution obtained from the LNO coupled cluster approach.

This procedure allows us to calculate CCSD(cT) estimates for the large molecules presented in the work of Hamdani *et al.* [11]. Therefore we calculate $\Delta = \text{CCSD}(T) - \text{CCSD}(cT)$ using the LNO-CCSD(T) results from Table S V together with Eq. 2. This energy difference Δ is subtracted from the the well-converged LNO-CCSD(T) estimates provided in Ref. [11].

We estimate the uncertainty of the CCSD(cT)-fit interaction energy as the sum of the LNO-CCSD(T) uncertainty provided in Ref. [11] and an uncertainty from the fit. The former is a consequence of the tightness parameters controlling the local approximation. The latter can simply be calculated via the standard deviation of the residuals σ , which provides an error estimate for X . In correspondence with the uncertainty of the DMC results, which take 2σ , our corresponding error estimate for $1/X$ is thus given by $2\sigma/X^2$. Hence, the uncertainty measure for the fit depends on the considered molecular system but roughly takes the value of $2\sigma/X^2 \approx 0.025$ for all considered cases. Finally, this leads to an error estimate of

$$\delta(\text{CCSD}(cT)\text{-fit}) = \delta(\text{LNO-CCSD}(T)) + \left| \frac{2\sigma}{X^2} \cdot \text{LNO-(T)} \right|. \quad (4)$$

In fact, we make the simplification that $\delta(\text{LNO-CCSD}(T))$ and $\delta(\text{LNO-CCSD})$ are similar, as only the former is provided in Ref. [11].

Table S IV. Interaction energies in kcal/mol of a set of dispersion-dominated complexes from the S22, L7 and S66 benchmark datasets. Systems from the S22 test set are taken from Table S II and are calculated using cc-pVDZ basis sets. Systems from the S66 are obtained from [34] extrapolation and were taken from Table S I. Results for the three molecules from the L7 test set are obtained from plane wave calculations and were taken from Table S III.

System	MP2 corr.	CCSD corr.	(T)	(cT)
Methane dimer	-0.619	-0.559	-0.064	-0.059
Ethene dimer	-1.797	-1.368	-0.244	-0.218
Benzene-Methane complex	-2.424	-1.810	-0.299	-0.260
Benzene dimer PD	-8.312	-5.361	-1.025	-0.849
Pyrazine dimer	-9.111	-5.685	-1.126	-0.930
Indolebenzene complex stack	-12.640	-8.028	-1.587	-1.308
Pyridine-Pyridine PD	-9.339	-5.794	-1.310	-1.080
Pyridine-Pyridine TS	-5.258	-3.597	-0.762	-0.642
Benzene-Pyridine PD	-9.052	-5.651	-1.282	-1.058
Benzene-Pyridine TS	-5.119	-3.488	-0.735	-0.618
Pyridine-Uracil PD	-10.701	-7.110	-1.637	-1.362
Benzene-Benzene PD	-8.665	-5.423	-1.234	-1.019
Benzene-Benzene TS	-5.194	-3.518	-0.748	-0.628
Uracil-Uracil PD	-11.525	-8.142	-1.972	-1.669
Benzene-Uracil PD	-10.982	-7.334	-1.670	-1.394
GGG	-12.245	-7.771	-1.384	-1.130
GCGC	-31.847	-21.193	-4.035	-3.343
C2C2PD	-54.561	-29.471	-7.702	-5.949

Table S V: Results for the L7 molecules and C₆₀[6]CPPA using the LNO-CCSD(T) algorithm in MRCC. We use aug-cc-pVTZ basis sets and employ counterpoise correction. In all calculations we use as LNO threshold the keyword Tight. Except for the C₆₀[6]CPPA molecule where we have employed the threshold Normal. CCSD and (T) correlation energy contain each half of the MP2 correction originating from weak pairs. In addition to the individual energy contributions we show our LNO-CCSD(T) results in comparison with the CBS estimates published in Ref. [11]. Δ is the estimated difference between (T) and (cT) based on the described fitting procedure.

System	HF	MP2 corr.	CCSD corr.	(T)	LNO-CCSD(T)	LNO-CCSD(T) [11]	Δ
GGG	8.160	-12.365	-8.380	-2.142	-2.362	-2.100	-0.337
GCGC	12.317	-30.221	-20.840	-5.305	-13.828	-13.600	-0.808
C2C2PD	15.974	-53.177	-29.888	-8.091	-22.005	-20.600	-1.725
C3A	9.291	-35.507	-20.709	-5.848	-17.266	-16.500	-1.181
PHE	-13.644	-11.463	-8.109	-2.641	-24.394	-25.400	-0.383
C3GC	17.486	-61.393	-36.794	-10.305	-29.614	-28.700	-1.996
C ₆₀ @[6]CPPA	56.349	-141.173	-78.777	-28.508	-50.936	-41.700	-6.142

- [1] M. Kállay, P. R. Nagy, D. Mester, Z. Rolik, G. Samu, J. Csontos, J. Csóka, P. B. Szabó, L. Gyevi-Nagy, B. Hégyel, I. Ladjánszki, L. Szegedy, B. Ladóczki, K. Petrov, M. Farkas, P. D. Mezei, and A. Ganyecz, *The Journal of Chemical Physics* **152**, 074107 (2020).
- [2] CC4S developer team, “CC4S user manual,” <https://manuals.cc4s.org/user-manual/> (2024).
- [3] B. D. L. Péter R. Nagy, László Gyevi-Nagy and M. Kállay, *Molecular Physics* **121**, e2109526 (2023).
- [4] M. Valiev, E. Bylaska, N. Govind, K. Kowalski, T. Straatsma, H. Van Dam, D. Wang, J. Nieplocha, E. Apra, T. Windus, and W. de Jong, *Comput. Phys. Commun.* **181**, 1477 (2010).
- [5] A. Irmmler, A. Gallo, and A. Grüneis, *The Journal of Chemical Physics* **154**, 234103 (2021), 2103.06788.
- [6] G. Kresse and J. Furthmüller, *Computational Materials Science* **6**, 15 (1996).
- [7] T. Gruber, K. Liao, T. Tsatsoulis, F. Hummel, and A. Grüneis, *Phys. Rev. X* **8**, 021043 (2018).
- [8] A. Grüneis, G. H. Booth, M. Marsman, J. Spencer, A. Alavi, and G. Kresse, *J. Chem. Theory Comput.* **7**, 2780 (2011).
- [9] F. Hummel, T. Tsatsoulis, and A. Grüneis, *The Journal of Chemical Physics* **146**, 124105 (2017).
- [10] G. Knizia, T. B. Adler, and H. J. Werner, *Journal of Chemical Physics* **130** (2009), 10.1063/1.3054300/908511.
- [11] Y. S. Al-Hamdani, P. R. Nagy, A. Zen, D. Barton, M. Kállay, J. G. Brandenburg, and A. Tkatchenko, *Nature Communications* **12**, 3927 (2021).